

1 **Mars Global Simulant MGS-1: A Rocknest-based open standard for**
2 **basaltic martian regolith simulants**

3 Kevin M. Cannon^{1,*}, Daniel T .Britt¹, Trent M. Smith², Ralph F. Fritsche², and Daniel
4 Batcheldor³

5 ¹University of Central Florida, Department of Physics, Orlando, Florida 32816

6 ²NASA Kennedy Space Center, Titusville, FL 32899

7 ³Florida Institute of Technology, Melbourne, FL 32901

8 *Corresponding author: cannon@ucf.edu

9 4111 Libra Drive

10 Physical Sciences Building 430

11 Orlando, FL 32816

12

13

14

15

16

17

18

19

20

21

22

23

24 **Abstract**

25 The composition and physical properties of martian regolith are dramatically
26 better understood compared to just a decade ago, particularly through the use of X-ray
27 diffraction by the Curiosity rover. Because there are no samples of this material on Earth,
28 researchers and engineers rely on terrestrial simulants to test future hardware and address
29 fundamental science and engineering questions. Even with eventual sample return, the
30 amount of material brought back would not be enough for bulk studies. However, many
31 of the existing regolith simulants were designed 10 or 20 years ago based on a more
32 rudimentary understanding of martian surface materials. Here, we describe the Mars
33 Global Simulant (MGS-1), a new open standard designed as a high fidelity mineralogical
34 analog to global basaltic regolith on Mars, as represented by the Rocknest windblown
35 deposit at Gale crater. We developed prototype simulants using the MGS-1 standard and
36 characterized them with imaging techniques, bulk chemistry, spectroscopy, and
37 thermogravimetric analysis. We found the characteristics of the MGS-1 based simulant
38 compare favorably to rover- and remote sensing-based observations from Mars, and offer
39 dramatic improvements over past simulants in many areas. Modest amounts of simulant
40 will be produced at the University of Central Florida. By publishing the mineral recipe
41 and production methods, we anticipate that other groups can re-create the simulant and
42 modify it as they see fit, leading to region-specific and application-specific versions
43 based on a common standard.

44

45

46

47 **1.0 Introduction**

48 Planetary materials available for laboratory study come from a handful of sample
49 return missions, as well as a large meteorite collection dominated by ordinary chondrites.
50 Because actual planetary samples tend to be rare and often expensive, various groups
51 have produced simulated planetary materials, or “simulants”, that aim to replicate one or
52 more features of a reference sample. These features commonly include the chemistry,
53 mineralogy, spectral properties, and geotechnical characteristics of rocks, regolith or fine
54 dust. Simulants have been used to test engineering hardware (e.g., Bernold, 1991), for
55 astrobiology studies (e.g., de Vera et al., 2004), and plant growth experiments (e.g.,
56 Wamelink et al., 2014), among other applications. However, past simulants (particularly
57 lunar ones) have been plagued by a lack of quality control (Taylor et al., 2016). Previous
58 simulants often sacrificed accuracy for convenience, had poor documentation, and the
59 resulting products have been assumed to be appropriate for all types of research. Perhaps
60 more problematic is that simulants have usually been produced in large batches, and
61 when the initial batch runs out it can be difficult to re-create the original material.

62 Simulants for martian regolith (informally, soil) are prone to these same issues,
63 and the most cited martian simulants have seen their supplies exhausted. The most
64 prominent Mars simulant is Johnson Space Center JSC Mars-1 (Allen et al., 1998), which
65 was later reproduced as JSC Mars-1A by Orbitec when the original supply ran out.
66 However, the Orbitec simulant website was taken down sometime in 2017 and it appears
67 that JSC Mars-1A is no longer available. The other notable Mars simulant is Mojave
68 Mars (MMS) (Peters et al., 2008), that is not currently available outside of NASA. An
69 education company called The Martian Garden sells two simulants that are reported to be

70 derived from the same source material as MMS, but in fact they have mined a highly
71 altered red cinder material instead of the original Saddleback Basalt (see below). The
72 utility of these simulants (JSC Mars-1, MMS, and their updated versions) comes mostly
73 from the fact that they are fine-grained, roughly basaltic composition materials: this may
74 be appropriate for certain uses that do not require high fidelity simulants, but
75 inappropriate for others.

76 The goal of this work is to develop an open standard for a martian regolith
77 simulant (Mars Global Simulant, MGS-1) with high fidelity in mineralogy, chemistry,
78 physical properties, and spectral properties compared to an appropriate reference
79 material, in this case the windblown soil Rocknest at Gale crater (Fig. 1a) (Bish et al.,
80 2013; Blake et al., 2013; Leshin et al., 2013; Minitti et al., 2013; Archer et al., 2014;
81 Sutter et al., 2017). We produced and analyzed prototype simulants (Fig. 1b) using this
82 standard, some of which are being used in soil remediation and plant growth studies for
83 future human exploration of Mars. Our group at UCF is building the capacity to produce
84 modest quantities of MGS-1 based simulant (tens to hundreds of kilograms) available to
85 the community at cost. However, as an open standard the same mineral recipe and
86 methods described below can be used to re-produce MGS-1 and modify it as desired
87 (§4.2).

88

89 *1.1 Previous Mars simulants*

90 JSC Mars-1 and MMS have been used in a variety of laboratory studies as “soil
91 simulants” (e.g., Shkuratov et al., 2002; de Vera et al., 2004; Arvidson et al., 2009; Zacny
92 et al., 2013), but these simulants are based on early studies of martian regolith. JSC Mars-

93 1 (Fig. 1c) was sourced from an altered palagonitic tephra from the Pu'u Nene cinder
94 cone between Mona Loa and Mona Kea in Hawaii (Allen et al., 1998). It consists almost
95 entirely of amorphous palagonitic material, with minor crystallites of plagioclase and
96 magnetite. JSC Mars-1 was designed as a spectral simulant, in that the nanophase iron
97 oxides (npOx) present in the altered Hawaiian tephra produced a good match to the
98 visible/near-infrared (VNIR) spectra from dusty deposits on Mars, particularly at shorter
99 wavelengths (Evans and Adams, 1979; Bell et al., 1993; Morris et al., 1993; Allen et al.,
100 1998; Morris et al., 2001).

101 MMS was designed as a geotechnical simulant and was sourced from the
102 Saddleback Basalt near the NASA Jet Propulsion Laboratory: it consists of crystalline
103 plagioclase, pyroxene, magnetite, and hematite, with trace ilmenite and olivine (Peters et
104 al., 2008). Although the original MMS is not available outside of NASA, The Martian
105 Garden company sells a product marketed as Mojave Mars Simulant, renamed MMS-1,
106 and an "enhanced" version, MMS-2 (Fig. 1d). MMS-2 is described as being spiked with
107 hematite, magnesium oxide, and unnamed sulfates and silicates. However, The Martian
108 Garden company had no contact with the creators of MMS, and their simulants do not
109 resemble the original version (compare Fig. 1d with Fig. 2 in Peters et al. (2008)). The
110 company is instead mining the highly altered red cinder material described by Beegle et
111 al. (2007) instead of the original Saddleback Basalt. Quantitative mineralogical analysis
112 is not available for either JSC Mars-1, MMS, MMS-1, or MMS-2, although this is not
113 really feasible for JSC Mars-1 due to its mostly amorphous character.

114 There are a number of important differences between these older Mars simulants
115 and new *in-situ* measurements of martian regolith. In terms of crystallinity, JSC Mars-1 is

116 almost completely amorphous, while MMS, MMS-1 and MMS-2 are nearly 100%
117 crystalline. In contrast, martian soils are a subequal mixture of crystalline and amorphous
118 phases, as revealed by the CheMin instrument on the Mars Science Laboratory (MSL)
119 (Bish et al., 2013; Dehouck et al., 2014). JSC Mars-1 is extremely hygroscopic, contains
120 >20 wt.% H₂O at ambient conditions, and is known to contain significant amounts of
121 organic matter as well. Most of the older simulant varieties contain almost no sulfur,
122 whereas martian regolith contains up to 6 wt.% SO₃ (assuming all S is in the form of
123 sulfate; Yen et al., 2005; Ming and Morris, 2017). As noted above, the MMS-2 simulant
124 is spiked with sulfates and other phases to resolve discrepancies in bulk chemistry, but
125 the composition on the package confusingly lists both mineral percentages and wt.%
126 oxides in the same table, summing them to 100%.

127 Other Mars simulants have also been developed based on terrestrial basalts,
128 natural weathering profiles, and commercial sand products. Nørnberg et al. (2009)
129 described Salten Skov 1, a magnetic dust analog mostly composed of crystalline iron
130 oxides. Schuerger et al. (2012) created a series of analog soils by spiking a terrestrial
131 basalt with various salts and carbonates; they used them to test the survival of microbial
132 colonies in martian conditions. Other countries have developed Mars simulants, including
133 a series of nepheline and quartz sands as geotechnical simulants for the European Space
134 Agency (Gouache et al., 2011), terrestrial basalt spiked with magnetite and hematite for
135 China's Mars exploration program (Zeng et al., 2015), and basalt mixed with volcanic
136 glass in New Zealand (Scott et al., 2017). These simulants have not yet been widely
137 distributed or adopted.

138

139 *1.2 New insights on martian regolith*

140 The surface of Mars is covered by an unconsolidated regolith produced by the
141 combined action of impact comminution, physical erosion by wind, water, and lava, and
142 chemical weathering by fluids and oxidants (mostly early in the history of Mars)
143 (McCauley, 1973; Malin and Edgett, 2000; Golombek and Bridges, 2000; Goetz et al.,
144 2005; Yen et al., 2005; Murchie et al., 2009). The finest particle size fraction, known as
145 dust, is lofted high into the atmosphere by winds and is implicated in global storm
146 patterns (Toon et al., 1977). Martian dust is somewhat chemically distinct from the
147 underlying soil, with a larger component of npOx responsible for its ochre hue (Morris et
148 al., 2001; Berger et al., 2016). Presumably the dust was or still is derived from regolith-
149 forming processes, such that martian dust is a more “processed” and oxidized version of
150 the underlying coarser soil. The soil itself has a basaltic composition (Yen et al., 2005;
151 Ming and Morris, 2017), derived from a globally basaltic crust (McSween et al., 2009).

152 Martian soils have been examined *in-situ* at seven locations by landers and rovers,
153 with supplemental information from orbital remote sensing. Soil major element chemistry
154 and mineralogy are quite similar at the Spirit, Opportunity, and Curiosity landing sites
155 (Yen et al., 2013; Ming and Morris, 2017), supporting the presence of a global basaltic
156 soil that may be locally to regionally enriched in rarer evolved volcanic compositions
157 (e.g., Christensen et al., 2005) or alteration phases (e.g., Squyres et al., 2008). However,
158 we note that the three landing sites compared in Yen et al. (2013) are all from sulfur-rich
159 terrains (Karunatillake et al., 2014), and a true global average may have less sulfur-
160 bearing minerals consistent with this bulk chemistry constraint. Regardless, the MGS-1
161 standard is modeled on the Rocknest windblown soil at Gale crater, with supplemental

162 information from measurements by other landed and orbital assets. Rocknest is the best-
163 characterized martian soil to date (Bish et al., 2013; Blake et al., 2013; Leshin et al.,
164 2013; Minitti et al., 2013; Archer et al., 2014; Sutter et al., 2017), and based on currently
165 available data its chemical similarity to soils at disparate landing sites makes it an
166 appropriate reference material from which to develop a new simulant standard.

167

168 **2.0 The MGS-1 standard**

169 *2.1 Design philosophy*

170 Our general approach to designing asteroid and planetary simulants is to start
171 from the mineralogy, because minerals are the basic building blocks of planetary
172 materials. Simulants designed to match bulk chemistry might provide a close match to
173 more readily available measurements (from Alpha Particle X-ray Spectrometer
174 instruments, for example), but a simulant could be designed from infinite combinations of
175 random compounds to reproduce the bulk chemistry of a reference material without
176 having any of the right minerals inside of it. By starting with the correct mineral
177 constituents, the derived properties (geotechnical, spectral, chemical, etc.) should fall out
178 of the final product, with adjustments made where necessary based on analyzing initial
179 prototypes. We applied this mineral-based design philosophy for the MGS-1 standard,
180 based on X-ray Diffraction (XRD) analyses for the crystalline portion of the Rocknest
181 soil (Bish et al., 2013), and inferences for the amorphous component (Bish et al., 2013;
182 Dehouck et al., 2014; Achilles et al. 2018).

183

184 *2.2 Mineral recipe and calculated bulk chemistry*

185 *2.2.1 Crystalline fraction*

186 The crystalline fraction of Rocknest is well constrained by XRD (Bish et al.,
187 2013). These measurements provide quantitative mass fractions of all minerals present at
188 ~1 wt.% or greater, and crystal chemistry constraints from unit cell parameters and/or site
189 occupancy. We adopt most of the same mineral proportions reported by Bish et al. (2013)
190 (Table 1), re-normalized for a 30% amorphous content that is intermediate between low
191 and high estimates of how much amorphous material is present (Bish et al., 2013;
192 Dehouck et al., 2014). The detected crystalline phases in Rocknest include plagioclase,
193 pyroxene, olivine, magnetite, anhydrite, hematite, ilmenite, sanidine, and quartz (Bish et
194 al., 2013). For simplicity and sourcing concerns we do not include ilmenite, sanidine or
195 quartz in the MGS-1 standard, which were near the detection limits of CheMin.
196 Magnetite, anhydrite and hematite were also near the detection limit, but magnetite is
197 important for magnetic properties, anhydrite for sulfur contents, and hematite for
198 pigmenting properties.

199

200 *2.2.2 Amorphous fraction*

201 Poorly crystalline and/or X-ray amorphous material makes up at least 21-22% of
202 the Rocknest soil sample by weight (Dehouck et al., 2014), and it is still not entirely clear
203 what this material is. Dehouck et al. (2014) and Morris et al. (2015) isolated the
204 elemental chemistry of the amorphous component using a mass balance approach (Table
205 2), showing that it is deficient in SiO₂, Al₂O₃, and CaO, and enriched in SO₃ and H₂O
206 compared to the bulk soil. The amorphous component likely cannot be explained by a
207 single phase, and is likely a mixture of npOx phases like ferrihydrite (Dehouck et al.,

208 2014; Dehouck et al., 2017), silica-bearing phases such as basaltic glass or opal, and one
209 or more sulfate species like ferric sulfate (Sklute et al., 2015) or sulfate anions adsorbed
210 onto other phases (McAdam et al., 2014; Rampe et al., 2016). Crystalline carbonates
211 were not detected in Rocknest, but evolved gas analysis suggests that one or more
212 carbonate-bearing phases is present (Sutter et al., 2017), such that a mixture could be
213 present, or the carbonates could be poorly crystalline. Other components not uniquely
214 detectable by XRD could include allophane, hisingerite, and gels/protoclays.

215 Despite this inherent uncertainty, we chose to represent the amorphous
216 component in the MGS-1 standard with materials for which there is independent
217 evidence, and/or whose combination approximates the derived chemistry (Dehouck et al.,
218 2014; Morris et al., 2015) of the Rocknest amorphous material. For MGS-1 this includes
219 basaltic glass, ferric sulfate, ferrihydrite, and iron carbonate. A least squares approach
220 was used to find the relative proportion of these phases that best reproduces the estimated
221 chemistry of the CheMin amorphous component. The goal was to include a parsimonious
222 and easy-to-source selection of phases that covered the major anion groups, instead of
223 including every possible amorphous material listed above. In terms of the silica-bearing
224 portion of the amorphous component, we note that glass on Mars has been severely
225 underappreciated in the past, and for some reason all but dismissed by some authors
226 interpreting the CheMin results. But glassy spherules are clearly observed in soils at both
227 the Phoenix and Curiosity landing sites (Goetz et al., 2010; Minitti et al., 2013), and the
228 widespread presence of glass is supported by recent orbital investigations (Horgan and
229 Bell, 2012; Cannon and Mustard, 2015; Cannon et al., 2017; Horgan et al., 2017). Indeed,
230 more recent detailed analysis of CheMin data suggest that basaltic glass makes up ~68%

231 of the amorphous material in Rocknest (Achilles et al. 2018), exactly in line with the
232 standard (Table 1). Ferric sulfate and iron carbonate, two of the four “amorphous”
233 species in MGS-1, are added to the prototype simulants in the crystalline state as iron
234 (III) sulfate pentahydrate and siderite, respectively. These species can be synthesized in
235 amorphous form by evaporating appropriate solutions in vacuum, but they are prone to
236 recrystallize in normal laboratory conditions.

237

238 *2.2.3 Oxychlorines and nitrates*

239 Oxychlorine species are also present in martian soil and could include
240 (per)chlorate salts (Hecht et al., 2009; Sutter et al., 2017) and/or peroxide species (Clancy
241 et al., 2004; Crandall et al., 2017). Nitrates are also present (Stern et al., 2015).
242 Perchlorates in particular have received significant attention because of their possible
243 toxicity, and they will present a challenge and opportunity for human exploration in the
244 future (Davila et al., 2013). No crystalline (per)chlorate salts were detected in Rocknest
245 above the ~1 wt.% detection limit, but evolved ClO_4 was detected (Archer et al., 2014).
246 This suggests that a mixture of such salts is likely present, or they are present as
247 amorphous/adsorbed species. We included crystalline nitrate and perchlorate salts in
248 some of our initial prototypes designed for agricultural studies, but do not include them in
249 the root MGS-1 standard.

250

251 *2.2.4 Elemental chemistry*

252 Because MGS-1 is a mineralogical standard, the bulk chemistry of simulants
253 created from the standard will change based on the crystal chemistry of the minerals

254 used. Table 2 lists the elemental chemistry of the bulk Rocknest soil and the isolated
255 amorphous component (Morris et al., 2015). In developing the mineral recipe, we
256 calculated an estimated chemical composition for MGS-1 simulants using the mineral
257 fractions in Table 1 and idealized chemical formulas for the constituent minerals,
258 including the actual Mars crystal chemistries for plagioclase, pyroxene and olivine from
259 Bish et al. (2013) and Morris et al. (2015). Average martian crust was used for the
260 basaltic glass composition (Taylor and McLennan, 2009). This results in an elemental
261 chemistry within ~2 wt.% of bulk Rocknest for all major oxide species. It can be difficult
262 to find large quantities of terrestrial minerals with crystal chemistries appropriate for
263 Mars, such that actual MGS-1 based simulants will deviate from the calculated chemistry
264 depending on the specific silicates used. More effort put into sourcing accurate mineral
265 chemistries (or combinations of endmembers) will result in a more accurate elemental
266 chemistry for the final product.

267

268 *2.2.5 Additional considerations*

269 Mars Global is not meant to be a perfect standard for simulants (if such a thing
270 exists), and there are almost certainly trace mineral species present in martian soil that
271 aren't represented in MGS-1: these could include phosphates, sulfides, chromates,
272 oxalates, and other rare species. Additional phases may be present in an amorphous or
273 poorly-crystalline state, as discussed above. As well, silicate minerals are likely shocked
274 to various degrees on Mars, whereas the basic MGS-1 standard does not account for this.
275 Some phases are detected in localized regions on Mars like opaline silica (Squyres et al.,
276 2008; Milliken et al., 2008), clays (Poulet et al., 2005), halide salts (Osterloo et al., 2008),

277 and potassic feldspar (Le Deit et al., 2016), and would be expected to be mixed into
278 regional soils, but likely not on a global scale at detectable (>1 wt.%) amounts. In §4.2
279 we discuss how different versions of MGS-1 could be created to simulate these regional
280 soils.

281

282 **3.0 Prototype simulant production**

283 Using the MGS-1 mineral standard, we created prototype regolith simulants and
284 analyzed them using a variety of instrumental techniques. The production methods and
285 results are described below.

286

287 *3.1 Source materials*

288 We have built up a large library of source minerals as part of ongoing work
289 developing high-fidelity asteroid simulants. These minerals have been crushed into
290 powders and analyzed by XRD, VNIR spectroscopy, and X-ray Fluorescence (XRF) to
291 verify their identity and detect any contaminants present. The source materials for the
292 MGS-1 prototypes come from a combination of these existing mineral stocks, newly
293 acquired stocks, and synthesized materials (ferrihydrite, and re-melted basaltic glass
294 fibers).

295 The crystal chemistry of the major silicates (plagioclase, pyroxene and olivine)
296 differs between the prototype simulants and actual Rocknest measurements. Unit cell
297 parameters for Rocknest minerals indicate $\sim\text{An}_{57}$ plagioclase (Bish et al., 2013), a
298 mixture of augite and pigeonite (Bish et al., 2013), and $\sim\text{Fo}_{40}$ olivine (Morris et al.,
299 2015). In the prototype simulants we used a sodic plagioclase from North Carolina, a

300 single bronzite-variety pyroxene from Brazil, and a highly forsteritic olivine from
301 Arizona. Natural, high-purity sources of fayalitic olivine, pigeonite, and unweathered
302 calcic plagioclase are rare on Earth, but efforts to source them in the future will greatly
303 improve the bulk chemistry of the simulants.

304

305 *3.2 Simulant preparation*

306 To create simulants using the MGS-1 standard, we mixed mineral components in
307 the proportions listed in Table 1. If the mineral powders are simply mixed together dry,
308 the resulting material will not accurately represent the properties of true martian regolith,
309 which consists of polymineralic grains of eroded basalt mixed with secondary minerals.
310 To address this, we used some of the same techniques for our asteroid simulants, where
311 polymineralic fused solid “cobbles” are created and then mechanically ground to achieve
312 a power law particle size distribution. To create these cobbles, the plagioclase, pyroxene,
313 olivine, basaltic glass, magnetite and hematite were combined (Fig. 2a) and mixed with
314 water and sodium metasilicate pentahydrate in a 100:20:2 ratio by weight. This mixture
315 was mechanically combined and kneaded to form a thick mud (Fig. 2b) that was then
316 placed in a microwave oven to fully remove the water (time and power settings depend
317 on the dimensions of the mud disk). Upon heating and drying, the sodium metasilicate
318 forms a polymer network that acts as a binder, such that the resulting cobbles are solid
319 and quite hard (Fig. 2c). These cobbles were then ground and mechanically mixed with
320 the remaining water-soluble phases (iron (III) sulfate, ferrihydrite, anhydrite, siderite) to
321 create the final simulant (Fig. 1b).

322 An alternative approach to create an MGS-1 based simulant would be to add the
323 mafic silicates as a pre-existing, unweathered olivine-rich basalt, or a combination of
324 unweathered ultramafic rocks that achieves roughly the correct combination of minerals.
325 However, sourcing this kind of material presents its own set of challenges, and usually
326 requires a large capital investment if the right material is not already being mined. The
327 other phases in the MGS-1 standard are available in relatively pure forms from either
328 natural sources or as synthetic chemical supplies.

329

330 *3.3 Analyses*

331 The prototype simulants were analyzed using a variety of imaging techniques and
332 bulk analyses. Results from these analyses were compared to relevant datasets from
333 various orbital and *in-situ* spacecraft measurements as appropriate.

334 The simulants were imaged using a JEOL JSM 6480 scanning electron
335 microscope (SEM) at the Materials Characterization Facility AMPAC at UCF to
336 characterize particle textures, and to assess the distribution of the re-mixed soluble phases
337 like ferrihydrite amongst the larger mostly silicate grains. The grain density of the
338 simulant was calculated by measuring the volume of a cold-pressed pellet using
339 displacement in acetone, and the bulk density was calculated by gently pouring loose
340 simulant into a graduated cylinder to measure its volume.

341 Bulk elemental chemistry of the simulant prototypes was measured at the
342 AMPAC using a PANalytical Epsilon XRF operating in oxides mode. Unpressed
343 powders were used, and the average of 5 analyses was taken. XRF has some difficulty
344 measuring Na and S; ideally, fused bead analysis on a microprobe or mass spectrometer

345 could be used in the future to more accurately measure bulk chemistry, but XRF
346 measurements are sufficient for the prototypes because the chemistry will change based
347 on the specific minerals used.

348 Spectral properties of the simulants were measured using an Analytical Spectrum
349 Devices FieldSpec spectroradiometer from 320 to 2550 nm. This range covers typical
350 measurements made by rovers and orbital remote sensing platforms at Mars. The JSC
351 Mars-1, MMS-1 and MMS-2 simulants were measured at the same time for comparison.
352 All the simulants were ground and dry-sieved to the same 45-75 μm size fraction.

353 Thermogravimetric analyses for the simulants were conducted with a TA
354 Instruments SDT Q600 instrument at the Kennedy Space Center. Approximately 8.5 mg
355 of simulant was heated to 1000 °C using a ramp rate of 30 °C/min, with the mass and
356 heat flow measured as a function of time. Historical TGA and/or evolved gas analysis
357 data are available for both JSC Mars-1 and MMS, and for Mars soils from the Phoenix
358 Thermal and Evolved Gas Analyzer (TEGA) instrument (Smith et al., 2009) and the MSL
359 Sample Analysis at Mars (SAM) instrument (Archer et al., 2014; Sutter et al., 2017).
360 However, these Mars data were acquired under lower pressures with different
361 atmospheric compositions and different ramp rates, such that care must be taken in
362 drawing direct comparisons. The Dynamic Albedo of Neutron (DAN) instrument on
363 Curiosity also provided information on near-surface hydrogen contents in Rocknest
364 materials (Jun et al., 2013).

365

366 **4.0 Results**

367 A photograph of the MGS-1 based simulant is shown in Fig. 1b, compared with
368 an approximately true color image of the Rocknest windblown soil (Fig. 1a) taken by the
369 MSL Mars Hand Lens Imager (Minitti et al., 2013). MGS-1 has a similar burnt umber
370 color to Rocknest, mostly caused by the mixture of gray to black silicates and the
371 ferrihydrite and hematite, which act as strong pigments. Fig. 3a shows a scanning
372 electron micrograph of the simulant grains, where the polymineralic nature is clearly
373 visible. Fig. 3b shows a closer view of the surface, where $\sim\mu\text{m}$ -sized flecks of ferrihydrite
374 and/or ferric sulfate are adsorbed onto the surface of a larger silicate grain.

375

376 *4.1 Physical properties*

377 The grain (or particle) density of the prototype simulant is 2.72 g/cm^3 , and the
378 bulk density for loosely deposited material is 1.23 g/cm^3 , which gives a porosity of 55%.
379 Using more accurate Fe- and Ca-rich silicate compositions would result in higher
380 densities. By comparison, soils at the Pathfinder landing site had an estimated bulk
381 density of $1.07\text{-}1.64/\text{cm}^3$ (Moore et al., 1999), and drift material at the Viking 1 landing
382 site had an estimated bulk density of $1.15\pm 0.15 \text{ g/cm}^3$ (Moore and Jakosky, 1989),
383 although the lower gravity may affect bulk density somewhat. We could not find a
384 published estimate of density or porosity for the Rocknest windblown soil. Pristine
385 martian basalts have much higher grain densities ($>3 \text{ g/cm}^3$), but this density would be
386 lowered through physical and chemical weathering processes during regolith formation.

387 The particle size distribution of simulants is highly adjustable through crushing
388 and sieving. For most of the prototypes we ground the material to a $<6.3 \text{ mm}$ grain size,
389 with a natural power-law size distribution created by crushing. The particle size

390 distribution for martian regolith is not well constrained, mostly due to camera resolution
391 limits. Pike et al. (2011) reported that ~1 vol. % of the Phoenix surface materials were <4
392 μm , but Ming and Morris (2017) estimate that due to chemical alteration, 15-25 wt.% of
393 typical soils should consist of clay-sized grains. However, these alteration phases may be
394 adsorbed onto larger grains, and it is not clear whether they should count as discrete
395 “particles” in the context of geotechnical properties. In the past, highly detailed sieving,
396 separation and recombination methods have been used to generate simulants that match
397 the geotechnical properties of lunar regolith (e.g., Jiang et al., 2011). This may become
398 possible in the future for Mars with more detailed analysis of natural martian regolith.

399

400 *4.2 Bulk chemistry*

401 Table 2 lists the measured bulk chemistry of the prototype simulants as measured
402 by XRF (rightmost column), in addition to the forward-calculated estimates for the MGS-
403 1 standard described above. As expected, there are deviations from the Rocknest
404 measurements due to the crystal chemistry of the silicate minerals used in the prototypes.
405 CaO, FeO and MgO are most affected. Other elements such as SiO₂, Al₂O₃, and SO₃ are
406 much closer to the measured values from Rocknest, and compare favorably to older
407 martian simulants. For future versions of MGS-1 simulants, the best way to achieve a
408 more accurate bulk chemistry will be to use a more calcic plagioclase and a more
409 fayalitic olivine, or to physically combine endmember phases in appropriate proportions.

410

411 *4.3 Spectral properties*

412 Fig. 4 shows the reflectance spectrum of the MGS-1 prototype simulant compared
413 to previous simulants, and to telescopic and orbital data from Mars. At shorter
414 wavelengths, the MGS-1 based simulant is similar in shape and albedo to the Rocknest
415 spectra acquired by Mastcam (Wellington et al., 2017). In particular, the absorptions and
416 shoulders are consistent between 400 and 1100 nm, associated with (1) Fe^{2+} - Fe^{3+} and Fe-
417 O charge transfer, and (2) Fe^{2+} crystal field splitting. At longer wavelengths, the simulant
418 spectrum is similar to low albedo regions on Mars imaged by the Observatoire pour la
419 Minéralogie, l'Eau, les Glaces, et l'Activité (OMEGA) orbital spectrometer (Milliken et
420 al. 2007). However, the negative spectral slope at wavelengths >1000 nm in the remote
421 data is not as strong in the simulant, and the simulant is brighter. These observed
422 differences may be caused by a combination of differences in crystal chemistry, the
423 specific amorphous compounds present on Mars, shock darkening, as well as the fact that
424 the simulant spectra were measured at ambient laboratory conditions.

425 The other Mars simulants measured, JSC Mars-1, MMS-1 and MMS-2, are not
426 close matches to Rocknest or low albedo terrains measured by OMEGA. JSC Mars-1 has
427 a significantly higher albedo than the remote measurements, with strong H_2O - and OH-
428 related absorptions at 1400 and 1900 nm. The MMS-1 and MMS-2 simulants from The
429 Martian Garden company have even higher albedos than JSC-Mars 1, and at shorter
430 wavelengths are dominated by the signature of hematite. All three of the other simulants
431 have significant structure from 1900-2500 nm indicative of multiple different alteration
432 phases present in significant amounts. We did not measure the original MMS simulant
433 described by Peters et al. (2008), but the spectra shown in their Fig. 4 (no absolute

434 reflectance scale) and in Beegle et al. (2007) do not resemble the MMS-1 or MMS-2
435 simulants, and are more representative of actual Mars materials.

436

437 *4.4 Thermogravimetric analysis*

438 Fig. 5 shows the TGA data for the prototype simulant. The simulant lost 3.4%
439 relative mass at low temperatures (<300 °C), likely from physisorbed or weakly bound
440 H₂O. An additional 4.5% mass is lost between 300 and 1000 °C, which could include
441 additional H₂O, but is likely dominated by SO₂ and CO₂ from the breakdown of
442 carbonates and sulfates in the simulant. In comparison, Allen et al. (1998) reported that
443 JSC Mars-1 lost 21.1 wt.% (mostly water) when heated to 600 °C, while Peters et al.
444 (2008) report that MMS lost 1.7 wt.% by 100 °C and 7.2 wt.% by 500 °C. The significant
445 and unrealistic water contents of JSC Mars-1 were cited as a motivating factor in
446 developing the original MMS simulant (Peters et al., 2008), and MMS has recently been
447 augmented further to achieve even more realistic volatile release patterns (Archer et al.,
448 2018).

449 The TEGA instrument did not detect low temperature water release in soil
450 samples at the Phoenix landing site (Smith et al., 2009), but did detect a minor H₂O
451 release starting at 295 °C and a major release starting at 735 °C. In contrast, the SAM
452 instrument detected a broad H₂O release in Rocknest starting at low temperatures, finding
453 2.0 ± 1.3 wt.% total evolved water averaged over four runs (Archer et al., 2014). This is
454 consistent with the 1.5 wt.% water equivalent hydrogen in the upper layer of Rocknest
455 materials measured by DAN (Jun et al., 2013). Overall, these data show that the MGS-1
456 and MMS simulants are both more hydrated than martian soils, but are much closer in

457 hydration to reality than is JSC Mars-1. The differences between the MGS-1 based
458 simulant and Rocknest could be due to hygroscopicity in a humid terrestrial atmosphere,
459 and the exact nature of the amorphous component in Rocknest is probably key to
460 understanding the unique water release patterns measured by SAM (Archer et al., 2018).
461 TGA data are not available for MMS-1 or MMS-2, but judging from their spectral
462 properties (Fig. 4) these simulants have significant water contents, possibly on par with
463 JSC Mars-1.

464

465 **5.0 Discussion**

466 Simulants created using the MGS-1 standard are superior to previous martian
467 simulants, and accurately capture advances in the understanding of real martian regolith
468 in the 10 years since MMS was described (Peters et al., 2008) and the 20 years since JSC
469 Mars-1 debuted (Allen et al., 1998). The high fidelity of MGS-1 simulants is made
470 possible by the mineralogy-based synthesis, where mostly pure, individual components
471 are mixed together from scratch. This is in contrast to previous simulants, where a
472 natural, roughly basaltic terrestrial material was found that superficially matched Mars in
473 terms of spectral or geotechnical properties. That is not to say these previous simulants
474 have no value, especially where applications only require a bulk granular material that
475 behaves somewhat similarly to actual regolith on Mars.

476

477 *5.1 Applications*

478 Simulants based on MGS-1 are appropriate to use for a variety of scientific and
479 engineering-based investigations, as well as for testing flight hardware and developing *in-*

480 *situ* resource utilization (ISRU) technology. For lunar simulants, NASA developed the
481 concept of a fit-to-use matrix (Schrader et al., 2010), where various simulants are
482 compared by describing applications for which they are or are not recommended. For
483 example, the highlands simulant NU-LHT-1D was not recommended for drilling studies
484 because of its fine particle size distribution, but was deemed appropriate for oxygen
485 production studies. A simulant fit-to-use matrix is more relevant for the Moon because of
486 the vast proliferation of different lunar simulants, at least 28 by our count (not including
487 later derivatives). The situation for Mars is different, with only a handful of formally
488 described simulants so far (<http://sciences.ucf.edu/class/planetary-simulant-database/>):
489 the most prominent of these (MMS and JSC Mars-1) are no longer available, and the
490 others have not yet been widely adopted. Nevertheless, without a formal fit to use table
491 we can still list the various strengths and weaknesses of the MGS-1 standard in terms of
492 different use cases.

493 MGS-1 simulants are most recommended in applications where mineralogy and
494 volatile contents are important controlling factors. These include ISRU technology
495 development, plant growth and astrobiology studies, human health assessments, and
496 recurring slope lineae experiments, among others. JSC Mars-1 is not recommended for
497 these applications because it has virtually none of the same minerals as actual Mars soil,
498 and its volatile content (>20 wt.% H₂O) is highly unrealistic. The original MMS
499 simulant, and some of the newer simulants (JMSS-1, UC Mars1) may be appropriate for
500 some of these cases where accurate mineralogy is not critical. However, we caution
501 against using MMS-1 or MMS-2 due to their lack of rigorous documentation and the
502 discrepancies between these and the original MMS, as described above.

503 MGS-1 simulants are also recommended in applications for testing flight
504 hardware such as drilling, where geotechnical properties are important. MGS-1 is
505 appropriate for these cases because the synthesis method produces a “regolith” of
506 polymineralic grains with an adjustable particle size distribution, instead of simply
507 mixing dry powders together. However, the geotechnical properties of actual martian
508 regolith are poorly constrained compared to returned lunar regolith that has been studied
509 extensively on Earth. As well, in the prototypes we did not control for detailed aspects
510 like particle shape that can be important in influencing geotechnical properties, and our
511 initial physical properties measurements in this study are limited. Thus, at this time we
512 can only say that MGS-1 based simulants can likely be made to be as appropriate or more
513 so for hardware testing compared to previous Mars simulants. Mojave Mars Simulant
514 was developed specifically for geotechnical applications (Peters et al. 2008), and if the
515 original version can be obtained it is recommended for these uses. Again, due to apparent
516 changes between MMS and MMS-1/2, we do not recommend these simulants. Newer
517 Mars simulants (JMSS-1, UC Mars1, ES-X) may also be appropriate for geotechnical
518 applications. In order to improve the usefulness of Mars simulants for flight hardware
519 tests, more detailed study of martian regolith physical properties are needed. Some of this
520 may come from the InSight and ExoMars missions, which will hammer and drill deep
521 into surface materials. In addition, it would be useful to conduct a rigorous testing and
522 inter-comparison of martian simulants for physical properties (including thermophysical
523 properties).

524 We do not recommend using MGS-1 simulants for detailed geochemical studies
525 such as aqueous alteration experiments. This is due to the uncertainty in the exact amount

526 and nature of the amorphous component in martian soils, and the difficulty in sourcing
527 silicates on Earth with crystal chemistries appropriate for Mars. For these types of
528 studies, it may be better to use pure minerals in experiments, and/or to rely on
529 geochemical modeling based on primary volcanic compositions from martian meteorites
530 or rover measurements. In theory it is possible to create a small amount of extremely high
531 fidelity regolith simulant that satisfies both mineral and chemical constraints
532 simultaneously, but as described above it is cost-prohibitive to make this kind of simulant
533 in large quantities accessible to the community.

534

535 *4.2 Availability and future development of MGS-1*

536 In the past, simulant production has followed a now predictable lifecycle: the
537 need for a specific simulant arose, a NASA center or private company produced an initial
538 large batch of the simulant, then eventually the batch ran out, or national interest in a
539 given planetary body faded and the simulant was discarded. Efforts may be made to re-
540 create the original material under a different name, but this can often be difficult if the
541 source material is no longer accessible.

542 With MGS-1, we hope to avoid some of these pitfalls and move toward a more
543 open and sustainable model for simulant development. This starts with the general
544 philosophy of the standard: MGS-1 essentially means any simulant created based on the
545 mineralogy of average basaltic regolith on Mars, as captured by the mineral recipe in
546 Table 1. While we have chosen to add the plagioclase, pyroxene and olivine separately in
547 our prototypes, they could also be added in the form of basalt or ultramafic rocks
548 provided the mineral proportions are accurate. The MGS-1 recipe can be updated in the

549 future based on new analyses (for example, refining the amorphous component; Achilles
550 et al., 2018) and exploration of new landing sites. In this way, there is no batch of MGS-1
551 to run out, but a general standard to follow. We intend to produce modest quantities of
552 MGS-1 based simulant and distribute it to the community at cost, but we also encourage
553 others to re-create the same types of simulant using a similar standard. Indeed, a group at
554 the Johnson Space Center is also developing a Rocknest-based version of the MMS
555 simulant to be used for ISRU development (Archer et al., 2018).

556 NASA developed the concept of “root” and “branch” simulants for the Moon,
557 where the root is a basic, well-characterized version of the simulant. Specialized branch
558 versions can be derived from the root, either by the manufacturer or by end users. MGS-1
559 will benefit from the same scheme, where the recipe in Table 1 forms the basic root, and
560 various branches can be created either by us or others. For example, clay-rich Noachian
561 regolith, or perchlorate and nitrate-bearing agricultural soils can be created by adding the
562 desired additional components to the root simulant. These may evolve into standardized
563 simulants with version numbers to achieve better consistency, instead of each individual
564 lab developing their own simulant recipe. We encourage others to develop branched
565 versions of MGS-1 and add modifiers to the name as they see fit.

566

567 **6.0 Conclusions**

568 We developed a new standard for a Mars simulant, MGS-1 Mars Global Simulant,
569 based on the Rocknest soil examined by the Curiosity rover. Unlike previous simulants
570 sourced from landscaping material, Mars Global is meant to be assembled *ab initio* from
571 pure components to provide an accurate match to the mineralogy of martian regolith. The

572 spectral properties, water content, and physical properties of prototype simulants based
573 on MGS-1 are similar to measurements of Rocknest and other soils on Mars, and are an
574 improvement over previous simulants. MGS-1 based simulants are recommended for a
575 variety of applications including ISRU development, agriculture/astrobiology studies, and
576 testing flight hardware. Modest amounts of simulant will be produced and made available
577 to the community at cost, but through an open source philosophy we encourage end users
578 to freely replicate and modify the MGS-1 standard using the recipe and procedure
579 described here.

580

581 **Acknowledgements**

582 The authors would like to thank Richard Blair and Katerina Chagoya for help
583 with ferrihydrite synthesis, Jim Mantovani and Kevin Grossman for running the TGA
584 experiments, and the AMPAC facility staff for help with instrumental analyses.

585

586 **References**

587 Achilles, C.N., Downs, G.W., Downs, R.T., Morris, R.V., Rampe, E.B., Ming, D.W.,
588 Chipera, S.J., Blake, D.F., Vaniman, D.T., Bristow, T.F., Yen, A.S., Morrison,
589 S.M., Treiman, A.H., Craig, P.I., Hazen, R.M., Tu, V.M., Castle, N., 2018.
590 Amorphous phase characterization through X-ray diffraction profile modeling:
591 Implications for amorphous phases in Gale crater rocks and soils. Lunar and
592 Planetary Science Conference, XLIX, 59 Abstract #2661.

593 Allen, C., Morris, R.V., Jager, K.M., Golden, D.C., Lindstrom, D.J., Lindstrom, M.M.,
594 Lockwood, J.P., 1998. Martian Regolith Simulant JSC Mars-1. Lunar and
595 Planetary Science Conference, XXIX, 29 Abstract #1690.

596 Archer Jr., P.D., Franz, H.B., Sutter, B., Arevalo Jr., R.D., Coll, P., Eigenbrode, J.L.,
597 Glavin, D.P., Jones, J.J., Leshin, L.A., Mahaffy, P.R., McAdam, A.C., McKay,
598 C.P., Ming, D.W., Morris, R.V., Navarro-González, R., Niles, P., Pavlov, A.,
599 Squyres, S.W., Stern, J.C., Steele, A., Wray, J. J., 2014. Abundances and
600 implications of volatile-bearing species from evolved gas analysis of the Rocknest
601 Aeolian deposit, Gale Crater, Mars. *J. Geophys. Res.* 119, 237-254.
602 doi:10.1002/2013JE004493.

603 Archer Jr., P.D., Hogancamp, J.V., Gruener, J.E., Ming, D.W., 2018. Augmenting the
604 Mojave Mars Simulant to more closely match the volatile content of global
605 martian soils based on Mars Science Laboratory results. Lunar and Planetary
606 Science Conference, XLIX, 47 Abstract #2806.

607 Arvidson, R.E., Bonitz, R.G., Robinson, M.L., Carsten, J.L., Volpe, R.A., Trebi-Ollennu,
608 A., Mellon, M.T., Chu, P.C., Davis, K.R., Wilson, J.J., Shaw, A.S., Greenberger,
609 R.N., Siebach, K.L., Stein, T.C., Cull, S.C., Goetz, W., Morris, R.V., Ming, D.W.,
610 Keller, H.U., Lemmon, M.T., Sizemore, H.G., Mehta, M., 2009. Results from the
611 Mars Phoenix Lander Robotic Arm experiment. *J. Geophys. Res.* 114, E00E02.
612 doi:10.1029/2009JE003408.

613 Beegle, L.W., Peters, G.H., Mungas, G.S., Bearman, G.H., Smith, J.A., Anderson, R.C.,
614 2007. Mojave Martian Simulant: A New Martian Soil Simulant. Lunar and
615 Planetary Science Conference, XXXVIII, 38 Abstract #2005.

616 Bell III, J.F., Morris, R.V., Adams, J.B., 1993. Thermally altered palagonitic tephra: A
617 spectral and process analog to the soil and dust of Mars. *J. Geophys. Res.*, 98,
618 3373-3385. doi:10.1029/92JE02367.

619 Berger, J.A., Schmidt, M.E., Gellert, R., Campbell, J.L., King, P.L., Flemming, R.L.,
620 Ming, D.W., Clark, B.C., Pradler, I., VanBommel, S.J.V., Minitti, M.E., Fairén,
621 A.G., Boyd, N.I., Thompson, L.M., Perrett, G.M., Elliott, B.E., Desouza, E.,
622 2016. A global Mars dust composition refined by the Alpha-Particle X-ray
623 Spectrometer in Gale Crater. *Geophys. Res. Lett.* 43, 67-75.
624 doi:10.1002/2015GL066675.

625 Bernold, L.E., 1991. Experimental Studies on Mechanics of Lunar Excavation. *J.*
626 *Aerospace Eng.* 4, 9. doi:10.1061/(ASCE)0893-1321(1991)4:1(9).

627 Bish, D.L., Blake, D.V., Vaniman, D.T., Chipera, S.J., Morris, R.V., Ming, D.W.,
628 Treiman, A.H., Sarrazin, P., Morrison, S.M., Downs, R.T., Achilles, C.N., Yen,
629 A.S., Bristow, T.F., Crisp, J.A., Morookian, J.M., Farmer, J.D., Rampe, E.B.,
630 Stolper, E.M., Spanovich, N., MSL Science Team, 2013. X-ray Diffraction
631 Results from Mars Science Laboratory: Mineralogy of Rocknest at Gale Crater.
632 *Science* 341, 1238932. doi:10.1126/science.1238932.

633 Blake, D.F., Morris, R.V., Kocurek, G., Morrison, S.M., Downs, R.T., Bish, D., Ming,
634 D.W., Edgett, K.S., Rubin, D., Goetz, W., Madsen, M.B., Sullivan, R., Gellert, R.,
635 Campbell, I., Treiman, A.H., McLennan, S.M., Yen, A.S., Grotzinger, J.,
636 Vaniman, D.T., Chipera, S.J., Achilles, C.N., Rampe, E.B., Sumner, D., Meslin
637 P.-Y., Maurice, S., Forni, O., Gasnault, O., Fisk, M., Schmidt, M., Mahaffy, P.,
638 Leshin, L.A., Glavin, D., Steele, A., Freissinet, C., Navarro-González, R., Yingst,

639 R.A., Kah, L.C., Bridges, N., Lewis, K.W., Bristow, T.F., Farmer, J.D., Crism,
640 J.A., Stolper, E.M., Des Marais, D.J., Sarrazin, P., MSL Science Team, 2013.
641 Curiosity at Gale Crater, Mars: Characterization and Analysis of the Rocknest
642 Sand Shadow. *Science* 341, 1239505. doi:10.1126/science.1239505.

643 Cannon, K.M., Mustard, J.F., 2015. Preserved glass-rich impactites on Mars. *Geology* 43,
644 635-638. doi:10.1130/G36953.1.

645 Cannon, K.M., Mustard, J.F., Parman, S.W., Sklute, E.C., Dyar, M.D., Cooper, R.F.,
646 2017. Spectral properties of Martian and other planetary glasses and their
647 detection in remotely sensed data. *J. Geophys. Res.* 122, 249-268.
648 doi:10.1002/2016JE005219.

649 Christensen, P.R., McSween Jr., H.Y., Bandfield, J.L., Ruff, S.W., Rogers, A.D.,
650 Hamilton, V.E., Gorelick, N., Wyatt, M.B., Jakosky, B.M., Kieffer, H.H., Malin,
651 M.C., Moersch, J.E., 2005. Evidence for magmatic evolution and diversity on
652 Mars from infrared observations. *Nature* 436, 504-509. doi:10.1038/nature03639.

653 Clancy, R.T., Sandor, B.J., Moriarty-Schieven, G.H., 2004. A measurement of the 362
654 GHz absorption line of Mars atmospheric H₂O₂. *Icarus* 168, 116-121.
655 doi:10.1016/j.icarus.2003.12.003.

656 Crandall, P.B., Góbi, S., Gillis-Davis, J., Kaiser, R.I., 2017. Can Perchlorates be
657 Transformed to Hydrogen Peroxide (H₂O₂) Products by Cosmic Rays on the
658 Martian Surface? *J. Geophys. Res.* 122, 1880-1892. doi:10.1002/2017JE005329.

659 Davila, A.F., Willson, D., Coates, J.D., McKay, C.P., 2013. Perchlorate on Mars: a
660 chemical hazard and a resource for humans. *Int. J. Astrobio.* 12, 321-325.
661 doi:10.1017/S1473550413000189.

662 de Vera, J.-P., Horneck, G., Rettberg, P., Ott, S., 2004. The potential of the lichen
663 symbiosis to cope with the extreme conditions of outer space II: germination
664 capacity of lichen ascospores in response to simulated space conditions. *Adv.*
665 *Space Res.* 33, 1236-1243. doi:10.1016/j.asr.2003.10.035.

666 Dehouck, E., McLennan, S.M., Meslin, P.-Y., Cousin, A., 2014. Constraints on
667 abundance, composition, and nature of X-ray amorphous components of soils and
668 rocks at Gale crater, Mars. *J. Geophys. Res.* 119, 2640-2657.
669 doi:10.1002/2014JE004716.

670 Dehouck, E., McLennan, S.M., Sklute, E.C., Dyar, M.D., 2017. Stability and fate of
671 ferrihydrite during episodes of water/rock interactions on early Mars: An
672 experimental approach. *J. Geophys. Res.* 122, 358-382.
673 doi:10.1002/2016JE005222.

674 Evans, D.L., Adams, J.B., 1979. Comparison of Viking Lander multispectral images and
675 laboratory reflectance spectra of terrestrial samples. *Proceedings of the 10th Lunar*
676 *and Planetary Science Conference*, 1829-1834.

677 Goetz, W., Bertelsen, P., Binau, C.S., Gunnlaugsson, H.P., Hviid, S.F., Kinch, K.M.,
678 Madsen, D.E, Madsen, M.B., Olsen, M., Gellert, R., Klingelhöfer, G., Ming,
679 D.W., Morris, R.V., Rieder, R., Rodinov, D.S., de Souza Jr., P.A., Schröder, C.,
680 Squyres, S.W., Wdowiak, T., Yen, A., 2005. Indication of drier periods on Mars
681 from the chemistry and mineralogy of atmospheric dust. *Nature* 436, 62-65.
682 doi:10.1038/nature03807.

683 Goetz, W., Pike, W.T., Hviid, S.F., Madsen, M.B., Morris, R.V., Hecht, M.H., Stauffer,
684 U., Leer, K., Sykulka, H., Hemmig, E., Marshall, J., Morookian, J.M., Parrat, D.,

685 Vijendran, S., Bos, B.J., El Maarry, M.R., Keller, H.U., Kramm, R., Markiewicz,
686 W.J., Drube, L., Blaney, D., Arvidson, R.E., Bell III, J.F., Reynolds, R., Smith,
687 P.H., Woida, P., Woida, R., Tanner, R., 2010. Microscopy analysis of soils at the
688 Phoenix landing site, Mars: Classification of soil particles and description of their
689 optical and magnetic properties. *J. Geophys. Res.* 115, E00E22.
690 doi:10.1029/2009JE003437.

691 Golombek, M.P., Bridges, N.T., 2000. Erosion rates on Mars and implications for climate
692 change: Constraints from the Pathfinder landing site. *J. Geophys. Res.* 105, 1841-
693 1853. doi:10.1029/1999JE001043.

694 Gouache, T.P., Patel, N., Brunskill, C., Scott, G.P., Saaj, C.M., Matthews, M., Cui, L.,
695 2011. Soil simulant sourcing for the ExoMars rover testbed. *Planet. Space Sci.* 59,
696 779-787. doi:10.1016/j.pss.2011.03.006.

697 Hecht, M.H., Kounaves, S.P., Quinn, R.C., West, S.J., Young, S.M.M., Ming, D.W.,
698 Catling, D.C., Clark, B.C., Boynton, W.V., Hoffman, J., DeFlores, L.P.,
699 Gospodinova, K., Kapit, J., Smith, P.H., 2009. Detection of Perchlorate and the
700 Soluble Chemistry of Martian Soil at the Phoenix Lander Site. *Science* 325, 64-
701 67. doi:10.1126/science.1172466.

702 Horgan, B., Bell III, J.F., 2012. Widespread weathered glass on the surface of Mars.
703 *Geology* 40, 391-394. doi:10.1130/G32755.1.

704 Horgan, B.H.N., Smith, R.J., Cloutis, E.A., Mann, P., Christensen, P.R., 2017. Acidic
705 weathering of basalt and basaltic glass: 1. Near-infrared spectra, thermal infrared
706 spectra, and implications for Mars. *J. Geophys. Res.* 122, 172-202.
707 doi:10.1002/2016JE005111.

708 Jiang, M., Li, L., Sun, Y., 2011. Properties of TJ-1 Lunar Soil Simulant. *J. Aerospace*
709 *Eng.* 25, 463-469. doi:10.1061/(ASCE)AS.1943-5525.0000129.

710 Jun, I., Mitrofanov, I., Litvak, M.L., Sanin, A.B., Kim, W., Behar, A., Boynton, W.V.,
711 DeFlores, L., Fedosov, F., Golovin, D., Hardgrove, C., Harshman, K., Kozyrev,
712 A.S., Kuzmin, R.O., Malakhov, A., Mischna, M., Moersch, J., Mokrousov, M.,
713 Nikiforov, S., Shvetsov, V.N., Tate, C., Tret'yakov, V.I., Vostrukhin, A., 2013.
714 Neutron background environment measured by the Mars Science Laboratory's
715 Dynamic Albedo of Neutrons instrument during the first 100 sols. *J. Geophys.*
716 *Res.* 118, 2400-2412. doi:10.1002/2013JE004510.

717 Karunatillake, S., Wray, J.J., Gasnault, O., McLennan, S.M., Rogers, A.D., Squyres,
718 S.W., Boynton, W.V., Skok, J.R., Ojha, L., Olsen, N., 2014. Sulfates hydrating
719 bulk soil in the Martian low and middle latitudes. *Geophys. Res. Lett.* 41, 7987-
720 7996. doi:10.1002/2014GL061136.

721 Le Deit, L., Mangold, N., Forni, O., Cousin, A., Lasue, J., Schröder, S., Wiens, R.C.,
722 Sumner, D., Fabre, C., Stack, K.M., Anderson, R.B., Blaney, D., Clegg, S.,
723 Dromart, G., Fisk, M., Gasnault, O., Grotzinger, J.P., Gupta, S., Lanza, N., Le
724 Mouélic, S., Maurice, S., McLennan, S.M., Meslin, P.-Y., Nachon, M., Newsom,
725 H., Payré, V., Rapin, W., Rice, M., Sautter, V., Treiman, A.H., 2016. The potassic
726 sedimentary rocks in Gale Crater, Mars, as seen by ChemCam on board Curiosity.
727 *J. Geophys. Res.* 121, 784-804. doi:10.1002/2015JE004987.

728 Leshin, L.A., Mahaffy, P.R., Webster, C.R., Cabane, M., Coll, P., Conrad, P.G., Archer
729 Jr., P.D., Atreya, S.K., Brunner, A.E., Buch, A., Eigenbrode, J.L., Flesch, G.J.,
730 Franz, H.B., Freissinet, C., Glavin, D.P., McAdam, A.C., Miller, K.E., Ming,

731 D.W., Morris, R.V., Navarro-González, R., Niles, P.B., Owen, T., Pepin, R.O.,
732 Squyres, S., Steele, A., Stern, J.C., Summons, R.E., Sumner, D.Y., Sutter, B.,
733 Szopa, C., Teinturier, S., Trainer, M.G., Wray, J.J., Grotzinger, J.P., MSL Science
734 Team, 2013. Volatile, Isotope, and Organic Analysis of Martian Fines with the
735 Mars Curiosity Rover. *Science* 341, 1238937. doi:10.1126/science.1238937.

736 Malin, M.C., Edgett, K.S., 2000. Sedimentary Rocks of Early Mars. *Science* 290, 1927-
737 1937. doi:10.1126/science.290.5498.1927.

738 McAdam, A.C., Franz, H.B., Sutter, B., Archer Jr., P.D., Freissinet, C., Eigenbrode, J.L.,
739 Ming, D.W., Atreya, S.K., Bish, D.L., Blake, D.F., Bower, H.E., Brunner, A.,
740 Buch, A., Glavin, D.P., Grotzinger, J.P., Mahaffy, P.R., McLennan, S.M., Morris,
741 R.V., Navarro-González, R., Rampe, E.B., Squyres, S.W., Steele, A., Stern, J.C.,
742 Sumner, D.Y., Wray, J.J., 2014. Sulfur-bearing phases detected by evolved gas
743 analysis of the Rocknest Aeolian deposit, Gale Crater, Mars. *J. Geophys. Res.*
744 119, 373-393. doi:10.1002/2013JE004518.

745 McCauley, J.F., 1973. Mariner 9 evidence for wind erosion in the equatorial and mid-
746 latitude regions of Mars. *J. Geophys. Res.* 78, 4123-4137.
747 doi:10.1029/JB078i020p04123.

748 McSween Jr., H.Y., Taylor, G.J., Wyatt, M.B., 2009. Elemental Composition of the
749 Martian Crust. *Science* 324, 736-739. doi:10.1126/science.1165871.

750 Milliken, R.E., Mustard, J.F., Poulet, F., Jouglet, D., Bibring, J.-P., Gondet, B., Langevin,
751 Y., 2007. Hydration state of the Martian surface as seen by Mars Express
752 OMEGA: 2. H₂O content of the surface. *J. Geophys. Res.* 112, E08S07.
753 doi:10.1029/2006JE002853.

754 Milliken, R.E., Swayze, G.A., Arvidson, R.E., Bishop, J.L., Clark, R.N., Ehlmann, B.L.,
755 Green, R.O., Grotzinger, J.P., Morris, R.V., Murchie, S.L., Mustard, J.F., Weitz,
756 C., 2008. Opaline silica in young deposits on Mars. *Geology* 36, 847-850.
757 doi:10.1130/G24967A.1.

758 Ming, D.W., Morris, R.V., 2017. Chemical, Mineralogical, and Physical Properties of
759 Martian Dust and Soil. Dust in the Atmosphere of Mars and Its Impact on Human
760 Exploration Workshop Abstract #6027.

761 Minitti, M.E., Kah, L.C., Yingst, R.A., Edgett, K.S., Anderson, R.C., Beegle, L.W.,
762 Carsten, J.L., Deen, R.G., Goetz, W., Hardgrove, C., Harker, D.E., Herkenhoff,
763 K.E., Hurowitz, J.A., Jandura, L., Kenney, M.R., Kocurek, G., Krezoski, G.M.,
764 Kuhn, S.R., Limonadi, D., Lipkaman, L., Madsen, M.B., Olson, T.S., Robinson,
765 M.L., Rowland, S.K., Rubin, D.M., Seybold, C., Schieber, J., Schmidt, M.,
766 Sumner, D.Y., Tompkins, V.V., Van Beek, J.J., Van Beek, T., 2013. MAHLI at
767 the Rocknet sand shadow: Science and science-enabling activities. *J. Geophys.*
768 *Res.* 118, 2338-2360. doi:10.1002/2013JE004426.

769 Moore, H.J., Jakosky, B.M., 1989. Viking Landing Sites, Remote-Sensing Observations,
770 and Physical Properties of Martian Surface Materials. *Icarus* 81, 164-184.
771 doi:10.1016/0019-1035(89)90132-2.

772 Moore, H.J., Bickler, D.B., Crisp, J.A., Eisen, H.J., Gensler, J.A., Haldemann, A.F.C.,
773 Matijevic, J.R., Reid, L.K., Pavlics, F., 1999. Soil-like deposits observed by
774 Sojourner, the Pathfinder rover. *J. Geophys. Res.* 104, 8729-8746.
775 doi:10.1029/1998JE900005.

776 Morris, R.V., Golden, D.C., Bell III, J.F., Lauer Jr., H.V., Adams, J.B., 1993. Pigmenting
777 agents in martian soils: Inferences from spectral Mössbauer, and magnetic
778 properties of nanophase and other iron oxides in Hawaiian palagonitic soil PN-9.
779 *Geochim. Cosmochim. Acta* 57, 4597-4609. doi:10.1016/0016-7037(93)90185-Y.

780 Morris, R.V., Golden, D.C., Ming, D.W., Shelfer, T.D., Jørgensen, L.C., Bell III, J.F.,
781 Graff, T.G., Mertzman, S.A., 2001. Phyllosilicate-poor palagonitic dust from
782 Mauna Kea Volcano (Hawaii): A mineralogical analogue for magnetic Martian
783 dust? *J. Geophys. Res.* 106, 5057-5083. doi:10.1029/2000JE001328.

784 Morris, R.V., Ming, D.W., Gellert, R., Vaniman, D.T., Bish, D.L., Blake, D.F., Chipera,
785 S.J., Morrison, S.M., Downs, R.T., Rampe, E.B., Treiman, A.H., Yen, A.S.,
786 Achilles, C.N., Archer Jr., P.D., Bristow, T.F., Cavanagh, P., Fendrich, K., Crisp,
787 J.A., Des Marais, D.J., Farmer, J.D., Grotzinger, J.P., Mahaffy, P.R., McAdam,
788 A.C., Morookian, J.M., MSL Science Team, 2015. Update on the Chemical
789 Composition of Crystalline, Smectite, and Amorphous Components for Rocknest
790 Soil and John Klein and Cumberland Mudstone Drill Fines at Gale Crater, Mars.
791 46th Lunar and Planetary Science Conference, XLVI, 46 Abstract #2622.

792 Murchie, S.L., Mustard, J., Ehlmann, B.L., Milliken, R.E., Bishop, J.L., McKeown, N.K.,
793 Noe Dobrea, E.Z., Seelos, F.P., Buczkowski, D.L., Wiseman, S.M., Arvidson,
794 R.E., Wray, J.J., Swayze, G., Clark, R.N., Des Marais, D.J., McEwen, A.S.,
795 Bibring, J.-P., 2009. A synthesis of Martian aqueous mineralogy after 1 Mars year
796 of observations from the Mars Reconnaissance Orbiter. *J. Geophys. Res.* 114,
797 E00D06. doi:10.1029/2009JE003342.

798 Nørnberg, P., Gunnlaugsson, H.P., Merrison, J.P., Vendelboe, A.L., 2009. Salten Skov 1:
799 A Martian magnetic dust analogue. *Planet. Space Sci.* 57, 628-631.
800 doi:10.1016/j.pss.2008.08.017.

801 Osterloo, M.M., Hamilton, V.E., Bandfield, J.L., Glotch, T.D., Baldrige, A.M.,
802 Christensen, P.R., Tornabene, L.L., Anderson, F.S., 2008. Chloride-Bearing
803 Materials in the Southern Highlands of Mars. *Science* 319, 1651-1654.
804 doi:10.1126/science.1150690.

805 Peters, G.H., Abbey, W., Bearman, G.H., Mungas, G.S., Smith, J.A., Anderson, R.C.,
806 Douglas, S., Beegle, L.W. 2008. Mojave Mars simulant—Characterization of a
807 new geologic Mars analog. *Icarus* 197, 470-479.
808 doi:10.1016/j.icarus.2008.05.004.

809 Pike, W.T., Staufer, U., Hecht, M.H., Goetz, W., Parrat, D., Sykulska-Lawrence, H.,
810 Vijendran, S., Madsen, M.B., 2011. Quantification of the dry history of the
811 Martian soil inferred from in situ microscopy. *Geophys. Res. Lett.* 38, L24201.
812 doi:10.1029/2011GL049896.

813 Poulet, F., Bibring, J.-P., Mustard, J.F., Gendrin, A., Mangold, N., Langevin, Y.,
814 Arvidson, R.E., Gondet, B., Gomez, C., 2005. Phyllosilicates on Mars and
815 implications for early martian climate. *Nature* 438, 623-627.
816 doi:10.1038/nature04274.

817 Rampe, E.B., Morris, R.V., Archer Jr., P.D., Agresti, D.G., Ming, D.W., 2016.
818 Recognizing sulfate and phosphate complexes chemisorbed onto nanophase
819 weathering products on Mars using in-situ and remote observations. *Am. Mineral.*
820 101, 678-689. doi:10.2138/am-2016-5408CCBYNCND.

821 Schrader, C.M., Rickman, D.L., McLemore, C.A., Fikes, J.C., 2010. Lunar Regolith
822 Simulant User's Guide. NASA Technical Memorandum 2010–216446, NASA
823 Marshall Space Flight Center, Ala.

824 Schuerger, A.C., Golden, D.C., Ming, D.W., 2012. Biototoxicity of Mars soils: 1. Dry
825 deposition of analog soils on microbial colonies and survival under Martian
826 conditions. *Planet. Space Sci.* 72, 91-101. doi:10.1016/j.pss.2012.07.026.

827 Scott, A.N., Oze, C., Tang, Y., O'Loughlin, A., 2017. Development of a Martian regolith
828 simulant for in-situ resource utilization testing. *Acta Astron.* 131, 45-49.
829 doi:10.1016/j.actaastro.2016.11.024.

830 Shkuratov, Y., Ovcharenko, A., Zubko, E., Miloslavskaya, O., Muinonen, K., Piironen,
831 J., Nelson, R., Smythe, W., Rosenbush, V., Helfenstein, P., 2002. The Opposition
832 Effect and Negative Polarization of Structural Analogs for Planetary Regoliths.
833 *Icarus* 159, 396-416. doi:10.1006/icar.2002.6923.

834 Sklute, E.C., Jensen, H.B., Rogers, A.D., Reeder, R.J., 2015. Morphological, structural,
835 and spectral characteristics of amorphous iron sulfates. *J. Geophys. Res.* 120, 809-
836 830. doi:10.1002/2014JE004784.

837 Smith, P.H., Tamppari, L.K., Arvidson, R.E., Bass, D., Blaney, D., Boynton, W.V.,
838 Carswell, A., Catling, D.C., Clark, B.C., Duck, T., DeJong, E., Fisher, D., Goetz,
839 W., Gunnlaugsson, H.P., Hecht, M.H., Hipkin, V., Hoffman, J., Hviid, S.F.,
840 Keller, H.U., Kounaves, S.P., Lange, C.F., Lemmon, M.T., Madsen, M.B.,
841 Markiewicz, W.J., Marshall, J., McKay, C.P., Mellon, M.T., Ming, D.W., Morris,
842 R.V., Pike, W.T., Renno, N., Staufer, U., Stoker, C., Taylor, P., Whiteway, J.A.,

843 Zent, A.P., 2009. H₂O at the Phoenix Landing Site. *Science* 325, 58-61.
844 doi:10.1126/science.1172339.

845 Squyres, S.W., Arvidson, R.E., Ruff, S., Gellert, R., Morris, R.V., Ming, D.W.,
846 Crumpler, L., Farmer, J.D., Des Marais, D.J., Yen, A., McLennan, S.M., Calvin,
847 W., Bell III, J. F., Clark, B.C., Wang, A., McCoy, T.J., Schmidt, M.E., de Souza
848 Jr., P.A., 2008. Detection of Silica-Rich Deposits on Mars. *Science* 320, 1063-
849 1067. doi:10.1126/science.1155429.

850 Stern, J.C., Sutter, B., Freissinet, C., Navarro-González, R., McKay, C.P., Archer Jr.,
851 P.D., Buch, A., Brunner, A.E., Coll, P., Eigenbrode, J.L., Fairen, A.G., Franz, H.
852 B., Glavin, D.P., Kashyap, S., McAdam, A.C., Ming, D.W., Steele, A., Szopa, C.,
853 Wray, J.J., Martín-Torres, F.J., Zorzano, M.-P., Conrad, P.M., Mahaffy, P.R.,
854 MSL Science Team, 2015. Evidence for indigenous nitrogen in sedimentary and
855 aeolian deposits from the Curiosity rover investigations at Gale crater, Mars.
856 *PNAS* 112, 4245-4250. doi:10.1073/pnas.1420932112.

857 Sutter, B., McAdam, A.C., Mahaffy, P.R., Ming, D.W., Edgett, K.S., Rampe, E.B.,
858 Eigenbrode, J.L., Franz, H.B., Freissinet, C., Grotzinger, J.P., Steele, A., House,
859 C.H., Archer Jr., P.D., Malespin, C.A., Navarro-González, R., Stern, J.C., Bell III,
860 J.F., Calef, F.J., Gellert, R., Glavin, D.P., Thompson, L.M., Yen, A.S., 2017.
861 Evolved Gas Analyses of Sedimentary Rocks and Eolian Sediment in Gale Crater,
862 Mars: Results of the Curiosity Rover's Sample Analysis at Mars (SAM)
863 Instrument from Yellowknife Bay to the Namib Dune. *J. Geophys. Res.* 122,
864 2564-2609. doi:10.1002/2016JE005225.

865 Taylor, S.R., McLennan, S.M. Planetary Crusts: Their Composition, Origin and
866 Evolution. Cambridge University Press.

867 Taylor, L.A., Pieters, C.M., Britt, D., 2016. Evaluations of lunar regolith simulants.
868 Planet. Space Sci. 126, 1–7. doi:10.1016/j.pss.2016.04.005.

869 Toon, O.B., Pollack, J.B., Sagan, C., 1977. Physical properties of the particles composing
870 the Martian dust storm of 1971-1972. Icarus 30, 663-696. doi:10.1016/0019-
871 1035(77)90088-4.

872 Wamelink, G.W.W., Frissel, J.Y., Krijnen, W.H.J., Verwoert, M.R., Goedhart, P.W.,
873 2014. Can Plants Grow on Mars and the Moon: A Growth Experiment on Mars
874 and Moon Soil Simulants. PLoS ONE 9, e103138.
875 doi:10.1371/journal.pone.0103138.

876 Wellington, D.F., Bell III, J.F., Johnson, J.F., Kinch, K.M., Rice, M.R., Godber, A.,
877 Ehlmann, B.L., Fraeman, A.A., Hardgrove, C., MSL Science Team, 2017. Visible
878 to near-infrared MSL/Mastcam multispectral imaging: Initial results from select
879 high-interest science targets within Gale Crater, Mars. Am. Mineral. 102, 1202-
880 1217. doi:10.2138/am-2017-5760CCBY.

881 Yen, A.S., Gellert, R., Schröder, C., Morris, R.V., Bell III, J.F., Knudson, A.T., Clark,
882 B.C., Ming, D.W., Crisp, J.A., Arvidson, R.E., Blaney, D., Brückner, J.,
883 Christensen, P.R., DesMarais, D.J., de Souza Jr., P.A., Economou, T.E., Ghosh,
884 A., Hahn, B.C., Herkenhoff, K.E., Haskin, L.A., Hurowitz, J.A., Joliff, B.L.,
885 Johnson, J.R., Klingelhöfer, G., Maden, M.B., McLennan, S.M., McSween, H.Y.,
886 Richter, L., Rieder, R., Rodinov, D., Soderblom, L., Squyres, S.W., Tosca, N.J.,

887 Wang, A., Wyatt, M., Zipfel, J., 2005. An integrated view of the chemistry and
888 mineralogy of martian soils. *Nature* 436, 49-54. doi:10.1038/nature03637.

889 Yen, A.S., Gellert, R., Clark, B.C., Ming, D.W., King, P.L., Schmidt, M.E., Leshin, L.,
890 Morris, R.V., Squyres, S.W., Spray, J., Campbell, J.L., MSL Science Team, 2013.
891 Evidence for a Global Martian Soil Composition Extends to Gale Crater. *Lunar*
892 *and Planetary Science Conference*, XLIV, 44 Abstract #2495.

893 Zacny, K., Paulsen, G., McKay, C.P., Glass, B., Davé, A., Davila, A.F., Marinova, M.,
894 Mellerowicz, B., Heldmann, J., Stoker, C., Cabrol, N., Hedlund, M., Craft, J.,
895 2013. Reaching 1 m Deep on Mars: The Icebreaker Drill. *Astrobiology* 13, 1166-
896 1198. doi:10.1089/ast.2013.1038.

897 Zeng, X., Li, X., Wang, S., Li, S., Spring, S., Tang, H., Li, Y., Feng, J., 2015. JMSS-1: a
898 new Martian soil simulant. *Earth, Planets and Space* 67. doi:10.1186/s40623-015-
899 0248-5.

900

901

902

903

904

905

906

907

908

909

910 Table 1. Mineral recipe for the MGS-1 standard.
911

Component	Proportion (wt. %)
<i>Crystalline phases</i>	
Plagioclase	29.4
Pyroxene	20.5
Olivine	16.2
Magnetite	1.5
Anhydrite	1.1
Hematite	0.8
<i>Amorphous phases</i>	
Basaltic Glass	20.0
Fe-sulfate ¹	6.0
Ferrihydrite	2.7
Fe-carbonate ²	1.9
Sum	100

912 ¹In the prototype simulants we added crystalline iron (III) sulfate pentahydrate.

913 ²In the prototype simulants we added crystalline siderite.

914

915

916

917

918

919

920

921

922

923

924

925

926

927

928

929

930

931

932

933

934

935

936

937

938

939

940 Table 2. Elemental chemistry.
941

Oxide	RN bulk ^a	Calc. MGS-1 ^b	RN amorph. ^a	Calc. MGS-1 amorph. ^c	Prototype MGS-1 ^d
SiO ₂	41.2	42.5	35.9	33.4	41.4
TiO ₂	1.1	–	1.4	–	0.2
Al ₂ O ₃	9.0	10.8	5.52	7.1	11.2
Cr ₂ O ₃	0.5	–	0.8	–	0.1
FeO _T	19.3	21.4	19.9	29.5	13.3
MnO	0.4	–	0.5	–	.1
MgO	8.3	10.2	8.6	6.1	14.2
CaO	7.0	6.2	4.6	4.7	2.2
Na ₂ O	2.6	2.0	3.0	2.0	4.3
K ₂ O	0.5	0.1	0.7	0.3	2.3
P ₂ O ₅	0.9	–	1.9	–	0.3
SO ₃	5.2	3.6	9.9	10.0	8.9 ^e
H ₂ O	2.0	1.3	4.1	4.5	-
CO ₂	1.0	0.7	2.1	2.4	-
SUM	99.0	98.8	98.9	100.0	98.5

942 ^aFrom Morris et al. (2015). RN = Rocknest.

943 ^bCalculated bulk chemistry of MGS-1 using idealized mineral chemical formulas
944 weighted by the proportions in Table 1, with the actual crystal chemistries of martian
945 silicates from Bish et al. (2013) and Morris et al. (2015).

946 ^cHere, “amorphous” includes the basaltic glass, ferrihydrite, Fe-sulfate, and Fe-carbonate.

947 ^dAverage of 5 measurements.

948 ^eXRF has difficulty measuring sulfur accurately.

949

950

951

952

953

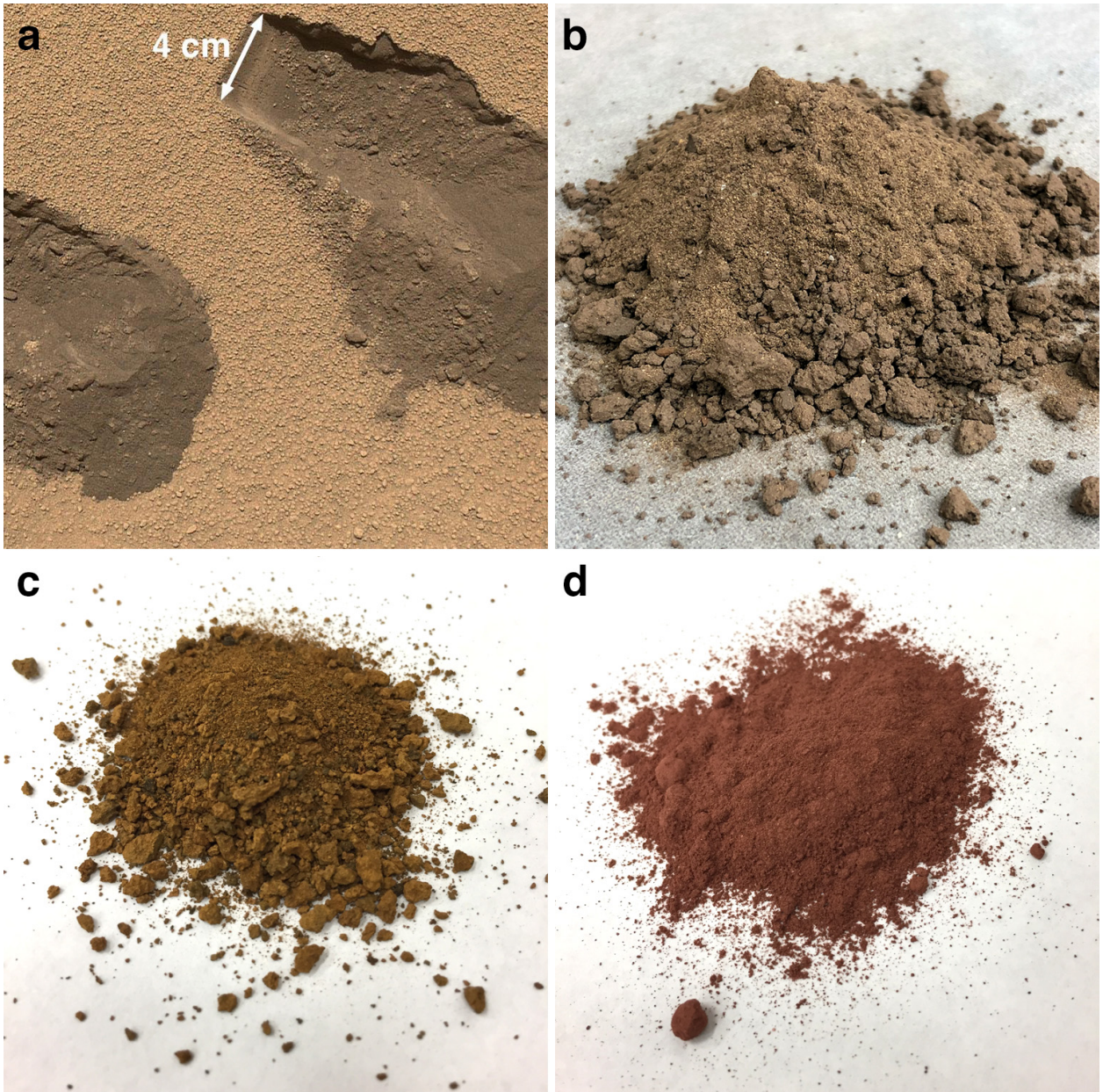
954

955

956

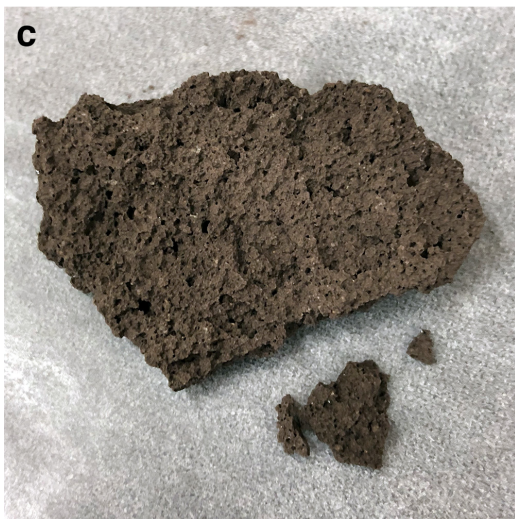
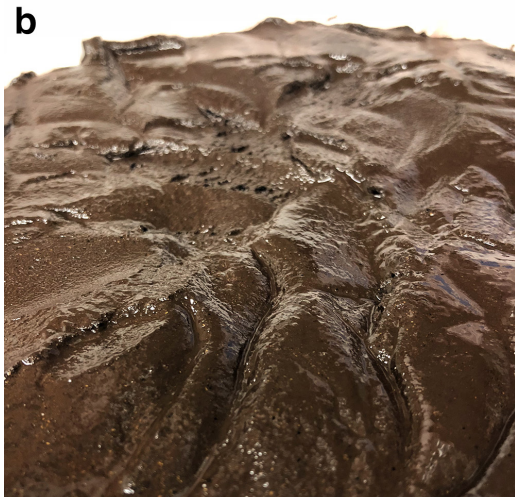
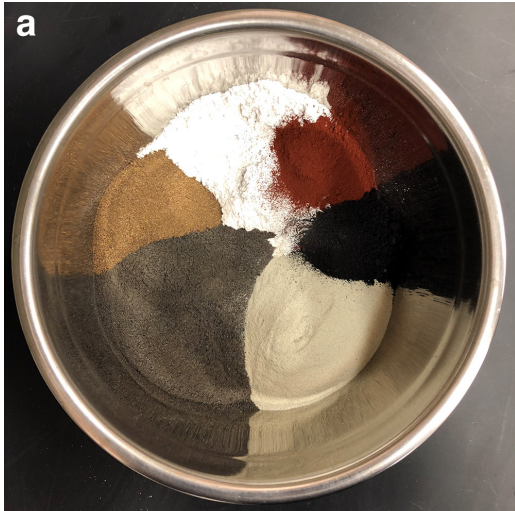
957

958



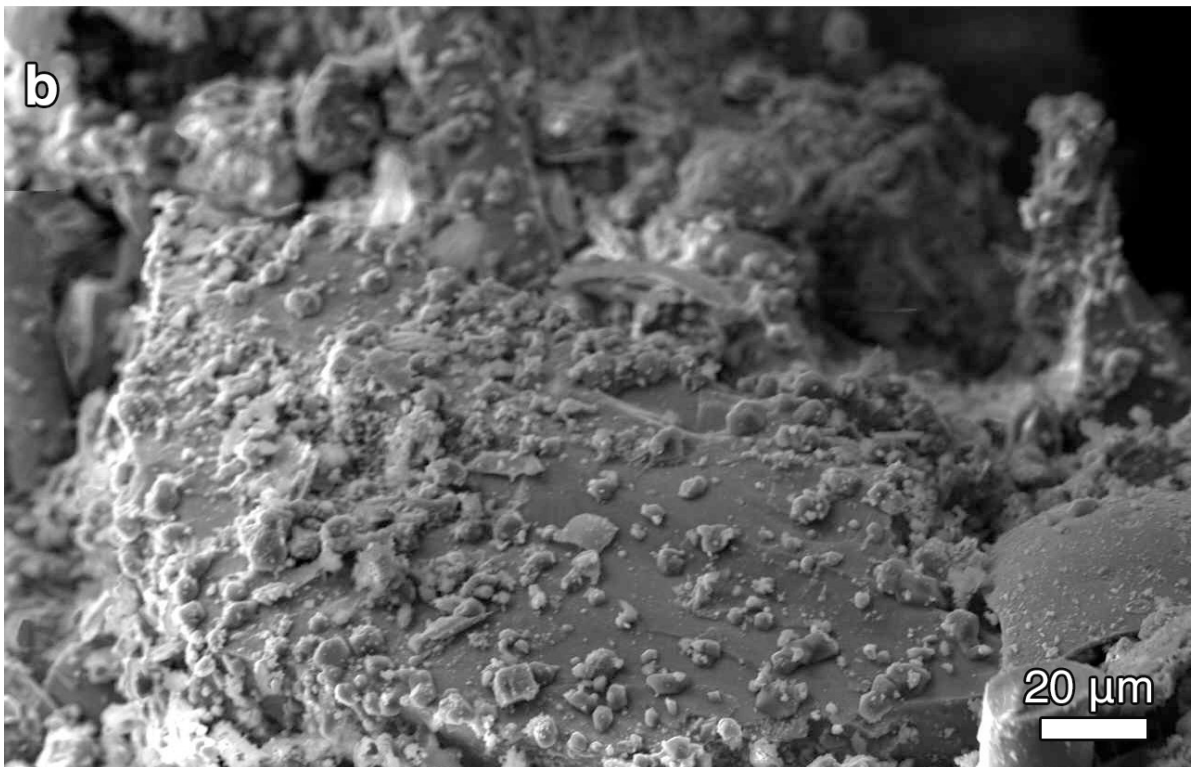
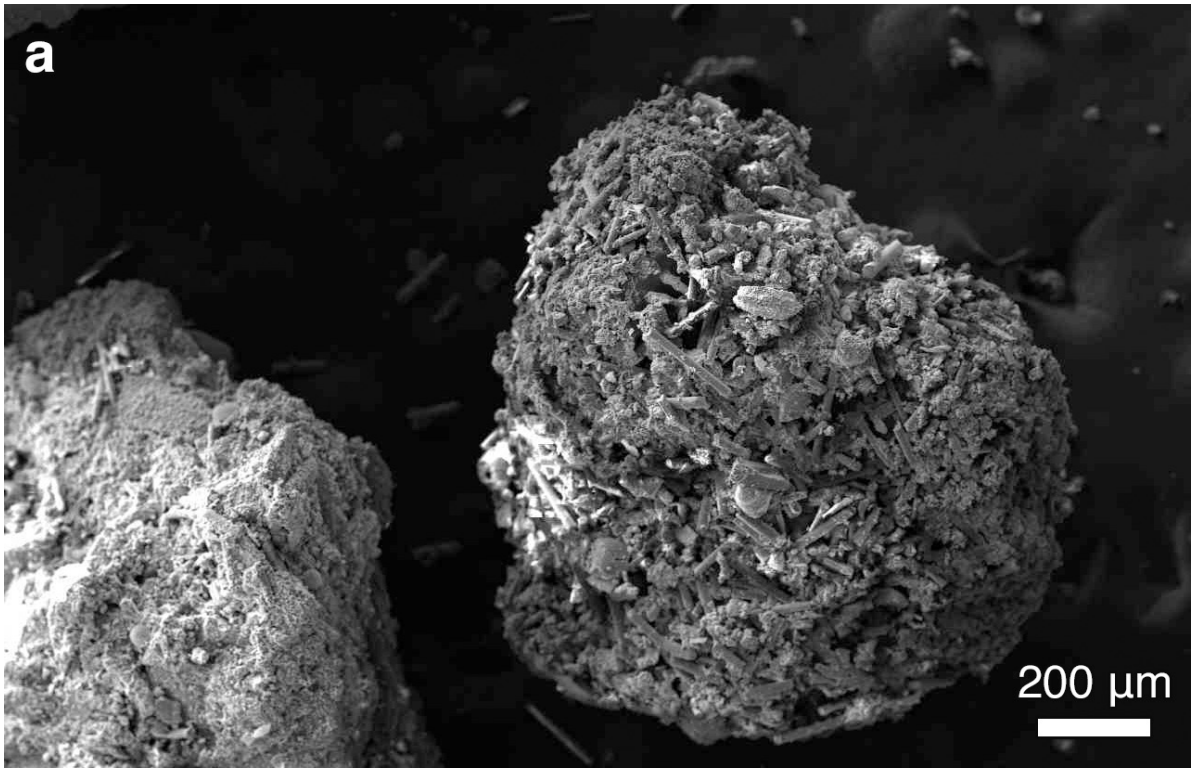
959
960
961
962
963
964
965
966
967
968
969
970
971
972

Figure 1. Comparison of martian simulants. a) MAHLI image of the scooped Rocknest soil; image credit NASA/JPL/Malin. b) Photograph of MGS-1 prototype simulant produced for this work. c) Photograph of JSC Mars-1. d) Photograph of MMS-2 sold by the Martian Garden company.



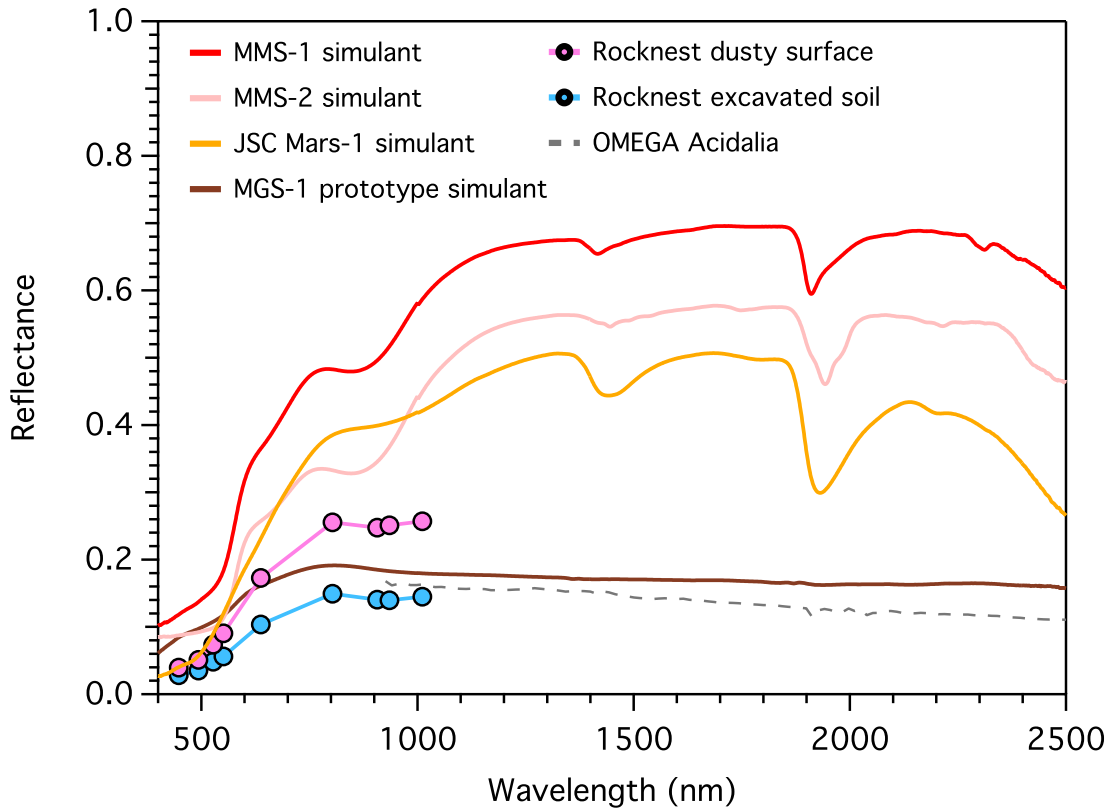
973
974
975
976
977

Figure 2. Production process for MGS-1 simulants. a) Insoluble ingredients before mixing. b) Thick mud paste formed from insoluble components, water, and sodium metasilicate. c) Resulting solid cobble formed after microwaving the mud.



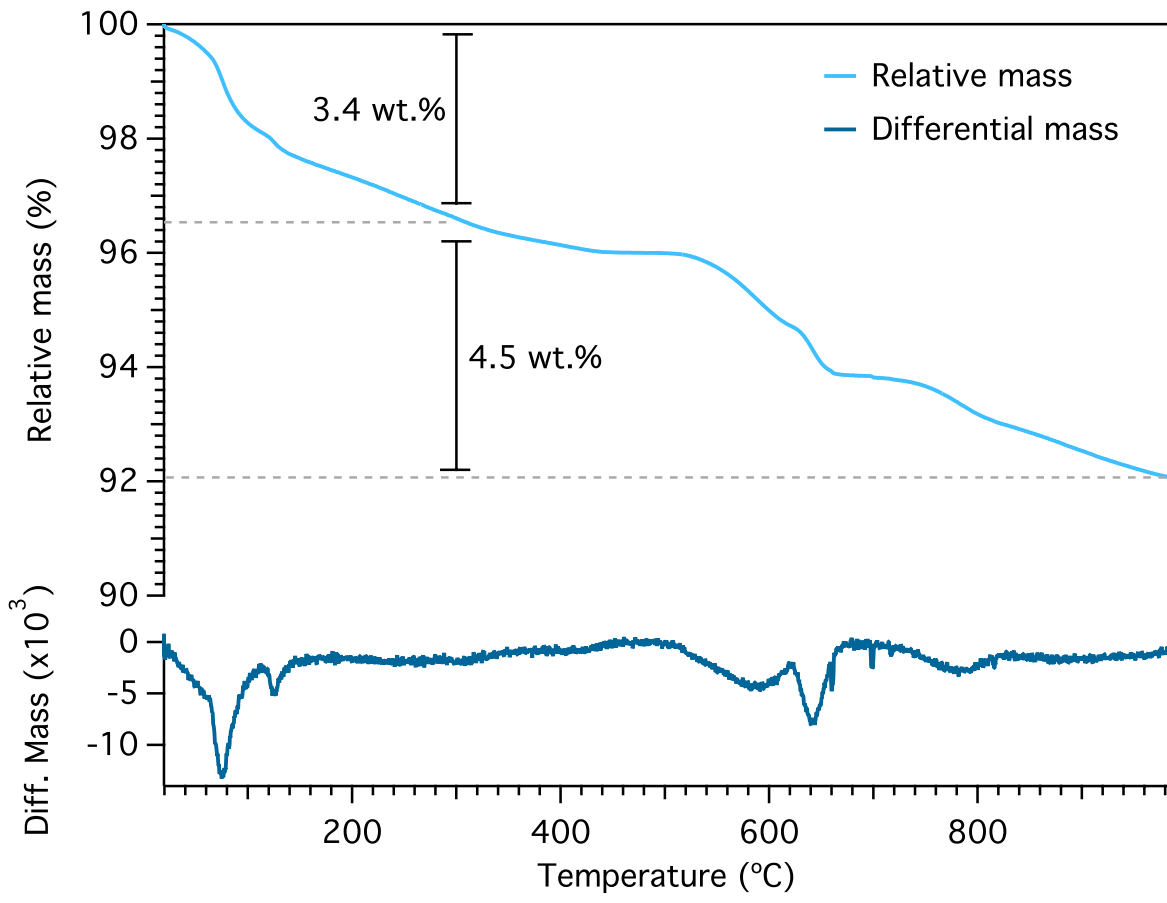
978
979
980
981
982
983

Figure 3. Scanning electron micrographs of MGS-1 prototype simulant grains. a) Zoomed out view showing polymineralic particles made up of multiple mineral constituents. b) Zoomed in view of the surface of a silicate grain covered with adsorbed ferrihydrite and/or ferric sulfate.



984
 985
 986
 987
 988
 989
 990

Figure 4. Spectral comparison of the MGS-1 simulant prototype, previous Mars simulants, and remotely sensed data from Curiosity and OMEGA. Mastcam data (filled circles) were reproduced from Fig. 5 in Wellington et al. (2017), and OMEGA data courtesy of R. Milliken. None of the spectra have been offset or scaled.



991
992
993
994
995
996
997

Figure 5. Thermogravimetric analysis of the MGS-1 prototype simulant.